Strongback System: A Way to Reduce Damage Concentration in Steel-Braced Frames

Jiun-Wei Lai[1] and Stephen A. Mahin, M.ASCE[2]

Abstract: This paper examines a newly developed seismic force-resisting system: the strongback system (SBS). To achieve improved seismic performance, this system combines aspects of a traditional concentric braced frame with a mast to form a hybrid system. The mast acts like a strong back to help resist the tendency of concentric braced frames to concentrate damage in one or a few stories during severe seismic excitations. The purpose of the strongback system is to promote uniform story drifts over the height of a structure. Three SBS prototypes were designed and analyzed considering a variety of earthquake excitations. Computed responses are compared with responses for three other braced frame systems. Results of quasi-static inelastic analyses, both monotonic and cyclic, are presented to demonstrate differences in the fundamental hysteretic behavior of the braced frame systems considered. A series of nonlinear dynamic response history analyses were then performed to compare the global and local dynamic response of each system. Results show that the SBS can effectively reduce the concentration of deformations using the proposed design strategy. Simplified cost analyses demonstrated the economic feasibility of incorporating the SBS for newly constructed buildings located in seismically active regions. **DOI: 10.1061/(ASCE)ST.1943-541X.0001198.**

Introduction

Conventional steel concentrically braced frames are prone to forming a soft-story mechanism (Khatib et al. 1988; Rai and Goel 1997; Sabelli 2001; Tremblay 2003; Hines and Appel 2007; Uriz and Mahin 2008; Hines et al. 2009; Lai et al. 2010; Chen and Mahin 2012) during strong earthquake ground shaking. This concentration of deformations in one or a few stories intensifies damage to braces at these levels, leading to greater nonstructural and structural damage and premature rupture of the braces at these levels compared to systems having more uniform distribution of damage over height. The concentration of damage can amplify P-Δ effects, which can in turn increase lateral displacements in the softened story. Soft stories are also likely to result in significant residual displacements, which can be costly or infeasible to repair.

As such, it is desirable to enhance the ability of concentric braced frames to avoid concentration of deformations and damage in a few stories. If a system is able to mitigate soft or weak story behavior, the peak deformation demands on individual braces and maximum residual displacements might be reduced. Several approaches have been explored by various researchers to reduce damage concentration and achieve smaller residual displacement. These systems include: (1) dual systems, where a moment resisting frame (MRF) is used in addition to the braced frame (Foutch et al. 1987; Whittaker et al. 1990; Kiggins and Uang 2006), (2) zipper or vertical tie bar systems (Khatib et al. 1988; Tirca and Tremblay 2004; Yang et al. 2008, 2009, 2010; Stavridis and Shing 2010), (3) rocking/uplifting systems (Clough and Huckelbridge 1977; Kelly and Tsztoo 1977; Uriz and Mahin 2008; Deierlein et al. 2011), and (4) tied-truss, masted, or strongback systems (SBS) (Martini et al. 1990; Whittaker et al. 1990; Popov et al. 1992; Ghersi et al. 2000; Tremblay 2003; Tremblay and Merzouq 2004; Mahin and Lai 2008; Mar 2010).

This paper examines the concept of a hybrid strongback system extended from zipper frames (Khatib et al. 1988), tied eccentrically braced frames (Popov et al. 1992; Ghersi et al. 2000), and an elastic truss system (Tremblay 2003; Tremblay and Merzouq 2004; Mar 2010). The system presented introduces vertical tie bars over most of the height of a stacked chevron or double-story X-braced bay. These connect the locations where the diagonal braces intersect along the span of the beams. As illustrated in Fig. 1, segments of the augmented braced bay are proportioned to provide a continuous vertical truss that is designed to remain essentially elastic during levels of excitation where soft story mechanisms are likely to occur. This vertical truss provides an elastic strongback or mast that imposes a nearly uniform lateral deformed shape over the height of the structure (Fig. 1). The versatility of the SBS systems is twofold: (1) a pinned connection or fixed connection appropriately detailed to develop the required plastic rotations can be provided at the base of the strongback truss; and (2) the braces and beam outside of the strongback truss are sized and detailed to yield, and either conventional buckling or buckling restrained braces (BRBs) can be used in conjunction with the SBS system.

Several possible bracing configurations and strongback spines are shown in Fig. 2. With proper sizing of the strongback mast system, the designer may have greater flexibility in locating and orienting the braces that yield. This system is not limited to vertical trusses, and other essentially elastic systems, such as steel or reinforced concrete structural walls, large plate girders, and so on, could be used for the strongback mast. For braces with significant differences in tension and compression capacities, it is expected that the overall structural system for a structure would include two strongback bays along each frame line so that an

[1]Postdoctoral Researcher, Pacific Earthquake Engineering Research Center, Dept. of Civil and Environmental Engineering, Univ. of California, Berkeley, R126, Bldg. 454, 1301 South 46th St., Richmond, CA 94804 (corresponding author). E-mail: adrian.jwlai@berkeley.edu; adrian.jwlai@gmail.com; jwlai@outlook.com

[2]Byron L. and Elvira E. Nishkian Professor of Structural Engineering and Director of the Pacific Earthquake Engineering Research Center, Dept. of Civil and Environmental Engineering, Univ. of California, Berkeley, 777 Davis Hall, Berkeley, CA 94720. E-mail: mahin@berkeley.edu

Note. This manuscript was submitted on April 14, 2014; approved on September 25, 2014; published online on November 6, 2014. Discussion period open until April 6, 2015; separate discussions must be submitted for individual papers. This paper is part of the ***Journal of Structural Engineering***, © ASCE, ISSN 0733-9445/04014223(11)/$25.00.

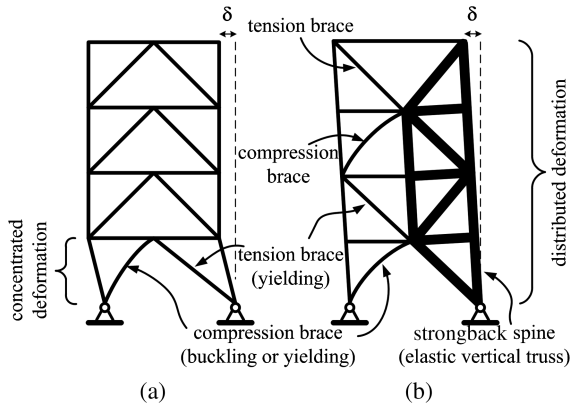

Fig. 1. Comparison of concentrically braced frame drifts: (a) without strongback concept; (b) with strongback concept

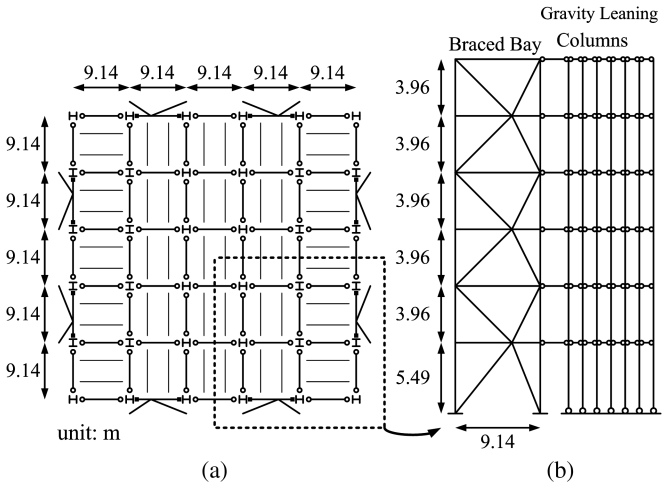

Fig. 3. Model building: (a) plan view; (b) 2D frame model elevation

equal number of yielding braces at a floor are loaded in tension and compression.

As shown in Fig. 2(d), the intersection of the braces at the floor beams can be shifted from the midspan of the beam, which can facilitate proportioning the load to various members in the SBS. In the cases considered herein, the vertical elastic truss portion of the bay is narrower than half the bay width, making the inelastic elements longer so that they have greater length over which to yield. Reducing the inclination of the inelastic braces has the benefit that they can be smaller yet able to resist the same lateral load on the structure. Moreover, for large lateral displacements of the frame, the increased length of the beam in the inelastic portion of the bay will be longer, reducing its shear and the plastic hinge rotations that might form at the ends of the beams.

The seismic behavior of SBS is evaluated by comparing the responses of three different SBS configurations with those of other braced frames having a more conventional arrangement of braces. Strongback bays with either conventional braces or BRBs are considered. In one of the cases examined, the steel cores for the BRBs are made of low-yield strength (LYS) steel. A range of ground motions was considered representative of the site for which the building models were designed. Nonlinear static pushover analyses (monotonic and cyclic) were carried out on each system to compare their basic mechanical characteristics. Nonlinear dynamic analysis results were compared to assess the ability of the SBS configuration

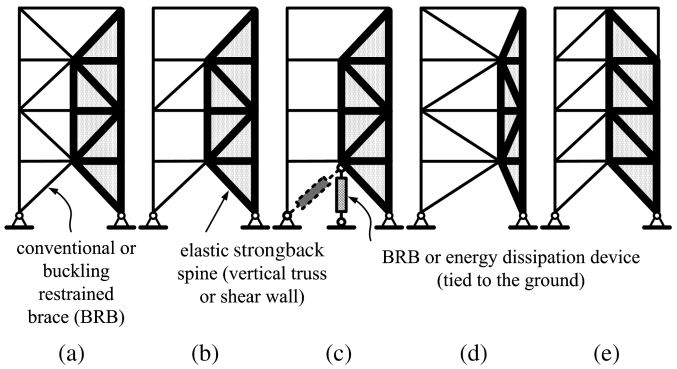

Fig. 2. Different strongback spine configurations with conventional braces or buckling restrained braces: (a) typical double-story X; (b) intermittent chevron; (c) tied-to-ground; (d) shifted double-story X; (e) chevron (inverted-V)

to minimize or eliminate soft story behavior and differences in behavior for the different systems considered. Comparisons of the cost estimates for the materials used for each system, and the local and global demand, were used to evaluate the SBS and develop recommendations for design and future research.

Model Building

A six-story model building was used to examine the behavior of SBS and other concentric braced frames. The basic model characteristics are shown in Fig. 3. Only the four braced bays in each direction were explicitly considered part of the lateral force-resisting system. The floor beams are assumed to have typical pin connections to the columns. Even though they are not part of the intended lateral load-resisting system, the gravity-only columns were included in the numerical models to approximate real conditions. Each direction has five beam spans and the bay widths are equal to 9.14 m. Each story is 3.96 m tall, except the ground story, which is 5.49 m high. The occupancy of the building is assumed to be that of a typical office building. The soil is designated Site Class D, and the building is located in downtown Berkeley, California. The building code used for the design of the model was ASCE 7-05 (ASCE 2005). Tributary dead load and live load were 100 and 50 psf, respectively. Live load was reduced where appropriate according to the provisions of ASCE 7-05. The seismic design coefficients considered are summarized in Table 1.

Table 1. Seismic Design Parameters

Design parameters	Values
Importance factor (I)	1.0
Seismic design category	D
Site class	D
Response modification factor (R)	6
System overstrength factor (Ω_o)	2.0
Deflection amplification factor (C_d)	5.0
S_1 (g)	0.787
S_S (g)	2.014
F_a	1.0
F_v	1.5
S_{D1} (g)	0.787
S_{DS} (g)	1.343

Seismic Force-Resisting Systems and Design Strategies

A total of six different configurations of seismic force-resisting systems were selected for this study (Fig. 4). A typical stacked chevron-bracing configuration was used as the benchmark, designated Model V6. The double-story split-X bracing configuration (Model X6) was selected as being representative of another typical configuration. A geometrically transformed model (Model X6-3) is basically the same as Model X6, but the intersection of the braces was shifted from the middle of the beam to the one-third point. Each direction of the prototype building had four braced bays with two at each perimeter face, as shown in Fig. 3(a). To ensure a symmetric lateral force-resisting system, the shifted points were aligned about the centerline of the elevation. That is, if one bay has a yielding/buckling braced inclined to the left, the other bay has the corresponding brace inclined to the right. Design of these three braced frame systems basically follows the ASCE 7-05 and the AISC seismic provisions (AISC 2005). System X6-3 was transformed to strongback system SB6-3 by incorporating vertical tie columns along the height of the braced bay from the second story to the fifth story. This completed the vertical spine.

In addition to the basic design requirements stipulated in ASCE 7-05 and the AISC seismic provisions, the members in the vertical elastic truss were designed to remain essentially elastic under design-level seismic forces. The simple design concept used here is based on the system code-specified over-strength factor, which is 2.0 in this case. Member stress checks were performed in SAP2000 (CSI 2009) using the load combinations listed in ASCE 7-05. Stress ratios in members within the vertical spine were specified to be less than 0.5, which is the reciprocal of the system over-strength factor for special concentrically braced frames. All tie columns were designed based on the maximum expected tension and compression brace forces that could develop. Although the vertical spine was designed to essentially remain elastic, it was expected that under severe ground shaking, some members in the vertical spine would be subjected to inelastic demands. One goal behind using this simple design strategy is to design a system that achieves the goal of preventing deformation concentration in the system at little increased cost. It is acknowledged that design optimization based on the performance goals is possible, but is outside the scope of this study.

The bracing members in Models V6, X6, X6-3, and SB6-3 were all conventional buckling braces. Hysteresis behaviors of braces are typically nonsymmetric and severe degradations of compression strengths are usually observed under cyclic loadings. Therefore, BRBs ($F_{y,brb} = 289.6$ MPa) are used in the SBS outside the vertical spine, as shown in Model SB6-3B in Fig. 4 since BRBs have nearly symmetric hysteresis loops and stable energy dissipation characteristics. Model SB6-3 L is essentially the same as Model SB6-3B, except the materials used in the steel cores of BRBs were composed of LYS steels ($F_{y,brb} = 103.4$ MPa). Lateral displacements in frames with BRBs are often larger than those for conventional braced frames since the area of steel in the braces is less, resulting in a more flexible system. By using LYS steel, more steel is required for the same strength, while the flexibility and period are reduced. Depending on the period range, this may further increase the amount of steel needed. The intent of using the LYS steel is to increase the stiffness and decrease the displacement of the system without increasing the strength too much. As LYS steel typically has lower yield-to-ultimate ratio compared with other grades of steel, this provides a buffer, redistributing the member forces to other members without failure. The design strategy of the vertical spines in Models SB6-3B and SB6-3 L was the same as for Model SB6-3. The selection procedures for the steel cores of the BRBs followed the Steel Tips report by Lopez and Sabelli (2004). The stiffness modification factors (due to the fact that BRB steel core cross-sectional area is not constant along the length of BRB) were taken as 1.3 for the first-story BRB and 1.4 for all other stories (Robinson 2009). These were applied in the structural analysis phase to account for the variation in steel core area from the yielding core to the enlarged attachment regions at the brace ends. Fig. 5 shows the details of braced bay member sizes for each model.

OpenSees Modeling

Two-dimensional computer models were developed in *OpenSees* (McKenna 1997; McKenna et al. 2010). Because of symmetry, only a quarter of the building was included in the analytical model. The braced bay was modeled and the gravity columns modeled

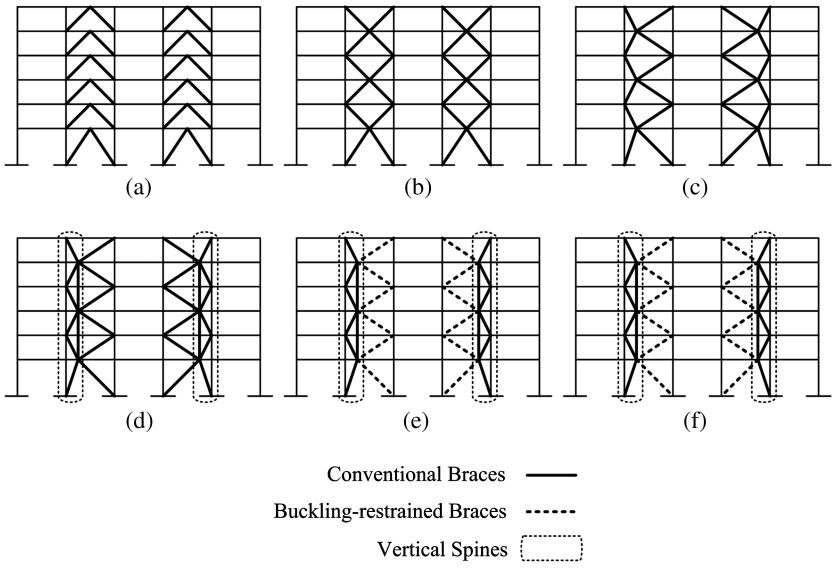

Fig. 4. Elevation views of six different bracing configurations: (a) V6; (b) X6; (c) X6-3; (d) SB6-3; (e) SB6-3B; (f) SB6-3 L

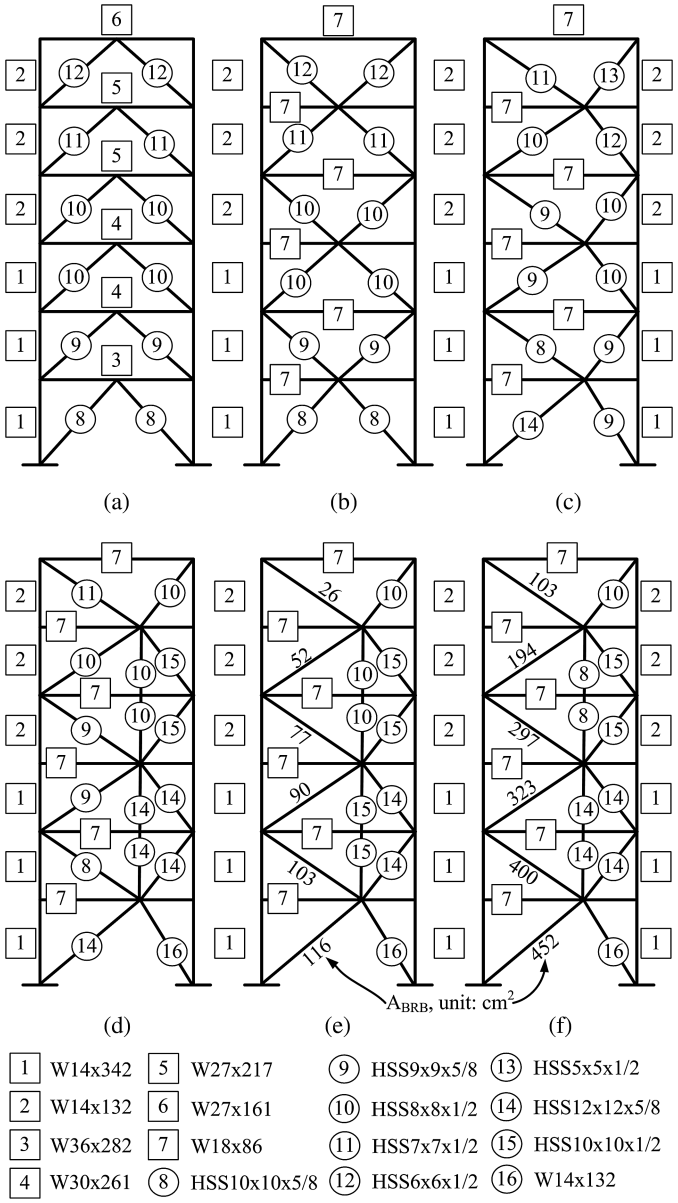

Fig. 5. Detail member sizes of each model: (a) V6; (b) X6; (c) X6-3; (d) SB6-3; (e) SB6-3B; (f) SB6-3 L

as leaning columns alongside the braced bay, as illustrated in Fig. 3(b). The leaning columns were pinned at the base and individually modeled for each gravity column line in *OpenSees*. All leaning columns were connected at each floor level using rigid links. Tributary gravity forces at each floor level were added for the corresponding nodal points of leaning columns. Both monotonic and cyclic quasi-static analyses, as well as nonlinear time history analyses, were performed for each structural system (Models V6, X6, X6-3, SB6-3, SB6-3B, and SB6-3 L). A Rayleigh damping parameter of 2% was used for both first and second modes for all six models. Initial imperfections equal to 1/1,000 of brace entire length were used in the models for all conventional buckling braces. Brace fracturing was modeled using Fatigue material in *OpenSees* (Uriz and Mahin 2008). Cyclic effects following Miner's rule were considered in this material type. Rigid end zones were applied at member ends based on the actual member sizes in the models. Pinned connections were assumed at every brace end. Both regular and LYS BRBs were modeled as pin-ended, two-node, force-based nonlinear beam-column elements with uniaxial

Table 2. Predefined Ground Motion Search Criteria

Criteria	Values
Magnitude (min)	5.0
Magnitude (max)	7.5
V_{S30} (m/s)	$182 \sim 366$
Fault type	Strike slip
Weighted period range (min ~ max)	$0.2T \sim 1.5T$
Scale factor	<3.0

Note: T is the fundamental period of the structure, $T = 0.6$ s.

material type Steel02 in *OpenSees*. The Steel02 material incorporates isotropic strain hardening, rather than kinematic hardening. Postelastic stiffness was assumed as 0.3% of elastic stiffness for both types of BRBs. Yield strengths of steel core materials were specified as 289.6 MPa for regular BRBs and 103.4 MPa for LYS BRBs.

Ground Motions

Five recorded ground motions were selected from the PEER Ground Motion Database (http://peer.berkeley.edu/peer_ground_motion_database/) for dynamic analysis. Each ground motion was selected using the online ground motion database searching tool with predefined record acceptance criteria (Table 2). Each record contained fault-normal, fault-parallel, and vertical components. Vertical components of ground motions were not included in this study. Ground motions were scaled to match the design earthquake (DE) and the maximum considered earthquake (MCE) response spectrums per ASCE 7-05. The scale factors of the ground motions were limited to be less than three. Each pair of ground motions is summarized in Table 3. Scaled average spectral acceleration of selected ground motion records are plotted in Fig. 6 with the DE response spectrum and MCE response spectrum.

Monotonic Pushover Results

Static pushover analyses were performed on the six models using *OpenSees*, with a control node at the roof level of the example building. The target displacement was set to be equal to 5% roof drift, which in this case corresponds to 1.27 m. An inverted triangle lateral force distribution was maintained during the pushover analyses. Monotonic pushover curves are shown in Fig. 7. Gravity forces were included in the analytical models.

The monotonic pushover curves in Fig. 7 show that the first four models (V6, X6, X6-3, and SB6-3) had similar initial stiffness. This is because the first four models have similar first mode periods as shown in Table 4. Models V6 and X6 had the same brace member sizes (Fig. 5) and thus had similar peak base shear capacity. Models X6-3 and SB6-3 had similar peak base shear capacity because of similar brace member sizes (Fig. 5) but these were about 10% higher than that found for Models V6 and X6. Once the brace at a certain floor level began to buckle, the base shear began to drop (for Models V6, X6, X6-3, and SB6-3). The base shear of Model V6 dropped after the brace at the first story buckled but later increased. With continued lateral displacement of Model V6, the unbalanced brace forces in the first story pulled down the center of the beam, and plastic hinges formed in the beam ends (beam-to-column connections were rigid connections). Later, plastic hinges formed in the columns, and the entire model developed a negative tangent stiffness at around 1.5% roof drift ratio. The beam-to-column connections were pinned (common connection details in practice) in Models X6, X6-3, and SB6-3; once a story

Table 3. Selected Ground Motions for Nonlinear Dynamic Response History Analysis

NGA number	Event	Year	Magnitude	Fault type	V_{S30} (m/s)	R_{rup} (km)	Scale factor, DE (MCE)
160	Imperial Valley-06	1979	6.53	Strike slip	223	2.7	0.88 (1.33)
1119	Kobe-Japan	1995	6.90	Strike slip	213	0.3	0.96 (1.44)
558	Chalfant Valley-02	1986	6.19	Strike slip	271.4	7.6	1.30 (1.95)
1853	Yountville	2000	5.00	Strike slip	271.4	11.4[a]	1.51 (2.26)
1602	Duzce-Turkey	1999	7.14	Strike slip	326	12	1.05 (1.57)

[a]R_{rup} with asterisk is estimated value.

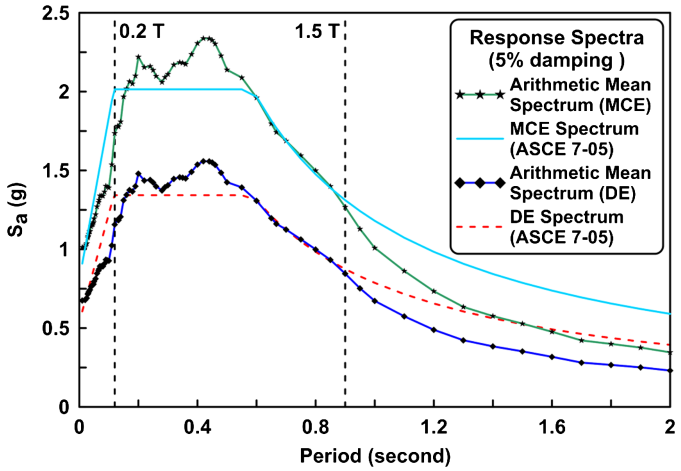

Fig. 6. Averaged spectrum of selected ground motion records

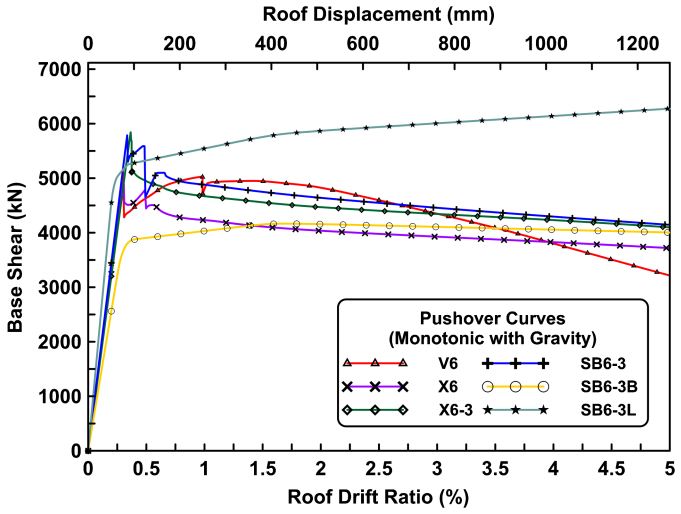

Fig. 7. Monotonic static pushover curves of six models

Table 4. First and Second Mode Periods of Each Model

Model name	First mode (s)	Second mode (s)
V6	0.69	0.25
X6	0.70	0.24
X6-3	0.70	0.25
SB6-3	0.67	0.24
SB6-3B	0.77	0.29
SB6-3 L	0.57	0.20

Table 5. Prescribed Roof Displacements for Cyclic Pushover Analyses

Sequence number	Number of cycle	Target roof displacement (mm)	Corresponding roof drift ratio (%)
1	2	±75.9	±0.3
2	2	±126.5	±0.5
3	2	±253	±1.0
4	2	±506	±2.0
5	2	±759	±3.0
6	2	±1,012	±4.0
7	2	±1,265	±5.0

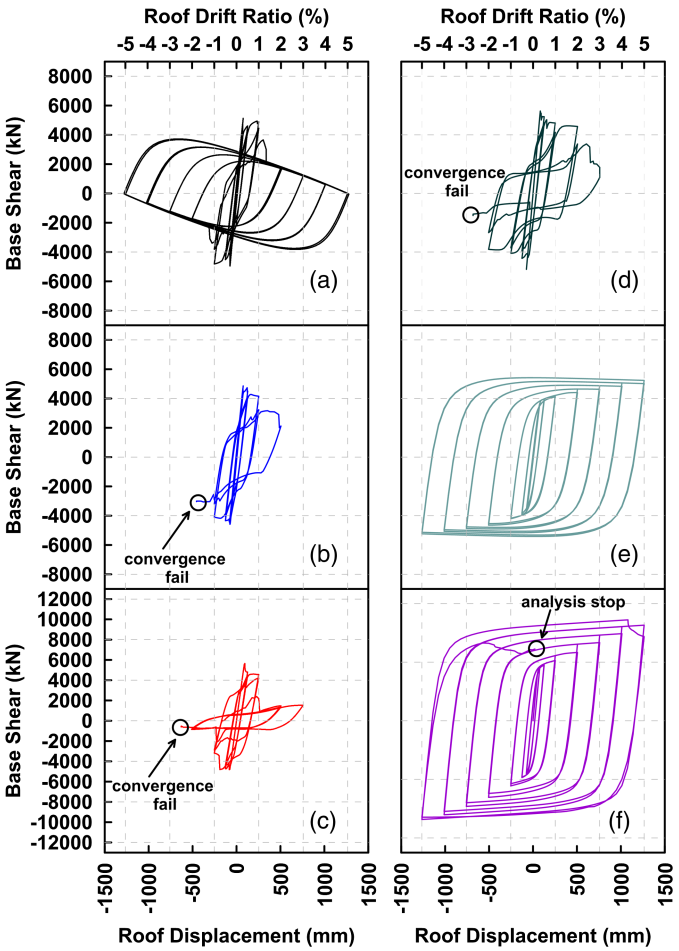

Fig. 8. Cyclic static pushover curves of six models: (a) V6; (b) X6; (c) X6-3; (d) SB6-3; (e) SB6-3B; (f) SB6-3 L

mechanism formed in these models, the base shear decreased gradually with increasing drift. The negative slopes for these models were smaller than for Model V6. The pushover curve of Model SB6-3 had several local peaks, indicating that braces other than first story buckled or yielded.

Table 6. Mean Responses of Each Model under Selected Ground Motions

Mean responses	Hazard level and ground motion component	V6	X6	X6-3	SB6-3	SB6-3B	SB6-3 L
Maximum base shear (kN)	DE, FN	5,337	5,661	6,026	6,442	4,747	6,181
	DE, FP	5,277	5,503	6,003	6,336	4,619	5,923
	MCE, FN	5,394	5,733	5,969	6,640	5,085	7,094
	MCE, FP	5,325	5,627	5,981	6,318	5,062	6,665
Maximum roof displacement (mm)	DE, FN	129.5	130.6	144.8	142.0	151.9	126.8
	DE, FP	158.2	165.6	169.7	163.8	194.3	136.9
	MCE, FN	200.7	206.3	206.3	225.0	222.5	168.4
	MCE, FP	284.2	280.9	287.0	324.6	272.3	218.2
Residual roof displacement (mm)	DE, FN	8.2	12.6	7.3	5.0	11.4	17.8
	DE, FP	8.9	22.8	14.9	40.3	28.2	22.4
	MCE, FN	18.5	44.9	40.2	28.3	35.7	19.0
	MCE, FP	51.6	66.2	39.1	59.6	41.5	40.0
Maximum column uplift force (kN)	DE, FN	9,442	8,996	10,519	10,466	6,994	10,162
	DE, FP	9,747	9,372	10,944	10,683	7,102	9,984
	MCE, FN	9,931	9,153	9,779	10,162	7,349	10,555
	MCE, FP	10,242	9,235	10,350	10,392	7,487	10,821
Maximum roof acceleration (g)	DE, FN	1.24	1.30	1.38	1.38	1.20	1.39
	DE, FP	1.21	1.17	1.26	1.18	1.17	1.16
	MCE, FN	1.64	1.56	1.63	1.60	1.59	1.82
	MCE, FP	1.53	1.53	1.52	1.66	1.61	1.56

Note: DE = design earthquake; MCE = maximum considered earthquake; FN = fault-normal; FP = fault-parallel.

Pushover curves of Models SB6-3B and SB6-3 L both exhibited a trilinear shape. Model SB6-3 L had a higher initial stiffness (due to larger brace steel core areas), while Model SB6-3B had lower initial stiffness compared to the other four models (due to its smaller brace steel core areas). The slope of the pushover curve of Model SB6-3 L never became negative. Model SB6-3B did exhibit a slightly negative slope when the roof drift ratio exceeded 1.8%.

Cyclic Pushover Results

In addition, cyclic pushover analyses were performed in *OpenSees* for all six models. The predefined cyclic target roof displacements are listed in Table 5 for all six models. Similar to monotonic pushover analyses, an inverted triangular lateral force distribution was applied during the cyclic loading. Fig. 8 shows the hysteretic curves including gravity effects for each model.

Quasi-static cyclic analyses show that the cyclic base shear capacity of Model V6 degraded more rapidly compared to the monotonic pushover analysis; the braces at the first story fractured at about 1.5% roof drift ratio, and the base shear capacity dropped to about zero at roof drift ratio, corresponding to 5%; see Fig. 8. Models X6, X6-3, and SB6-3 failed to complete the entire cyclic analysis protocol due to numerical convergence issues. Brace fracturing in Models V6, X6, X6-3, and SB6-3 was observed, as can be deduced from Fig. 8. Substantial cyclic hardening was observed in Models SB6-3B and SB6-3 L. Base shear capacity kept increasing in Model SB6-3 L, while in Model SB6-3B the base shear capacity very gradually decreased at larger roof displacements. Tie-column buckling of the six-story strongback system with conventional braces (Model SB6-3) was observed in the cyclic analyses; the small spike is noticeable in Fig. 8.

Clearly, the SBS with conventional braces or BRBs outperformed the braced frames with traditional bracing configurations.

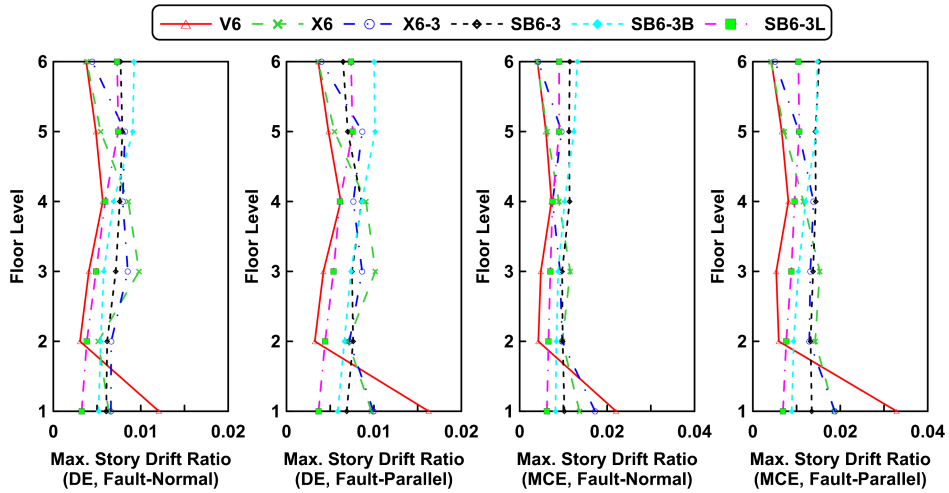

Fig. 9. Mean maximum story drift ratios (radian) for each model under DE and MCE level ground motions (with gravity columns)

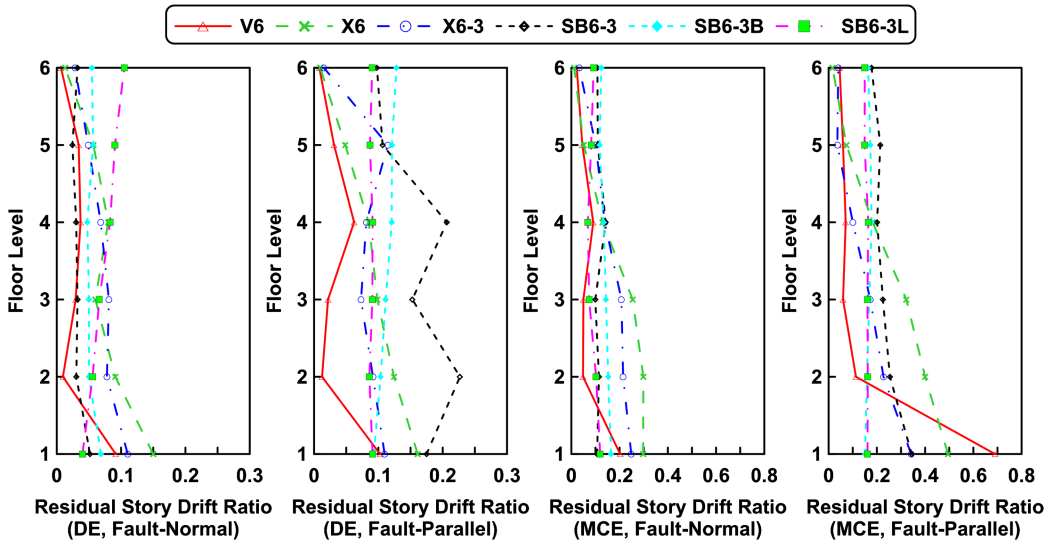

Fig. 10. Mean residual story drift ratios (radian) for each model under DE and MCE level ground motions (with gravity columns)

Using low-yield strength BRBs in the strongback hybrid system resulted in greater postyield deformation hardening than did the conventional BRBF.

Nonlinear Dynamic Response History Analysis Results

A total of 10 ground motions were used in the dynamic analysis. As mentioned earlier, ground motions were scaled to match DE and MCE response spectrums. Several dynamic response quantities were examined and summarized for each model. Table 4 shows the two highest periods for each model. The fundamental period of each model is larger than the design period of 0.55 s ($T = 0.02 \times 83^{0.75} = 0.55$) suggested by ASCE 7-05. Table 6 lists the mean responses of each model for the fault normal and fault parallel components of ground motions at DE and MCE levels.

As listed in Table 6, peak base shear forces were all between 4,600 and 7,100 kN. The order of peak base shear forces from dynamic analysis basically followed the order of the fundamental periods of six models: the lower the fundamental period, the higher the peak shear force. Maximum roof displacements under fault-parallel ground motions were all larger than the maximum roof displacements under fault-normal ground motions. The SBS with low-yield strength BRBs tended to have small roof displacements. The larger cross-sectional area of steel cores resulted in Model SB6-3 L being stiffer and stronger. As such, it tended to have smaller maximum roof displacements.

For the column base force demands, Model SB6-3B had the smallest column uplift forces among all six models—about 25% smaller—for the DE and MCE levels. The other five models had similar column uplift force demands.

As shown in Fig. 9, it is clear that a soft-ground-story formed in Model V6. Under the MCE-level event, this model exhibited a mean maximum drift ratio of more than 3%, which was concentrated at first story. Model X6 tended to form a soft two-story-panel mechanism.

It is interesting to note that slightly larger story drift ratios tended to occur in the upper stories of Models SB6-3, SB6-3B, and SB6-3 L compared to their lower stories. The distribution of story drift ratios of Model SB6-3 was close to a uniform pattern. The story drift ratios of Models SB6-3B and SB6-3 L had a very

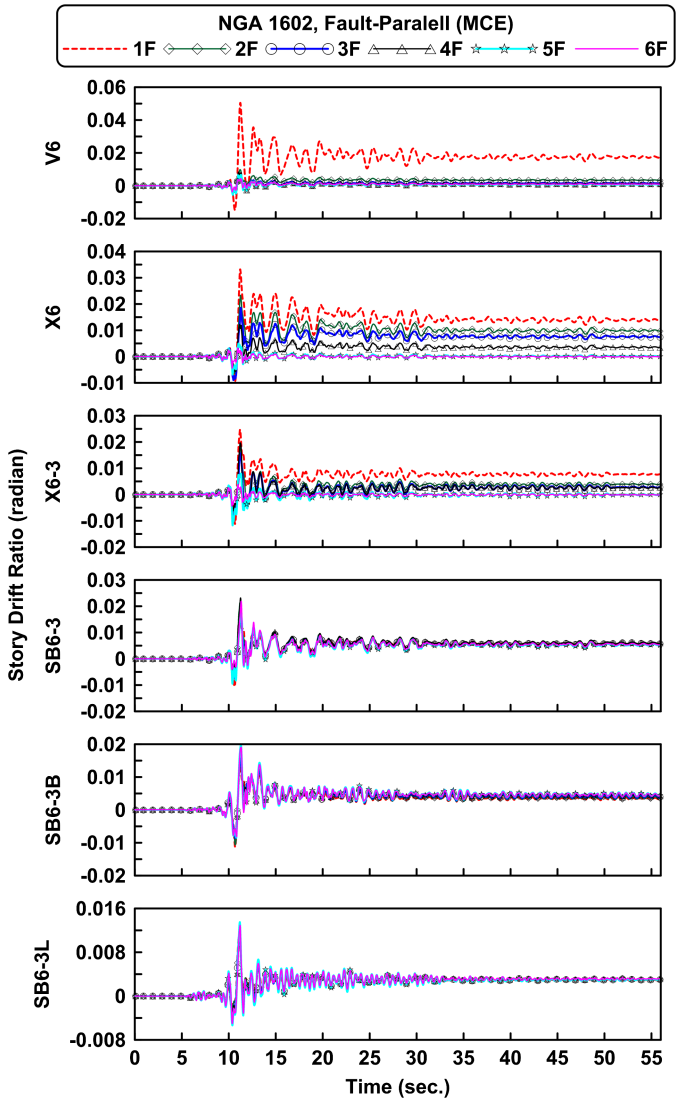

Fig. 11. Story drift ratio histories of six models under scaled NGA 1602 fault-parallel component ground motion (MCE level)

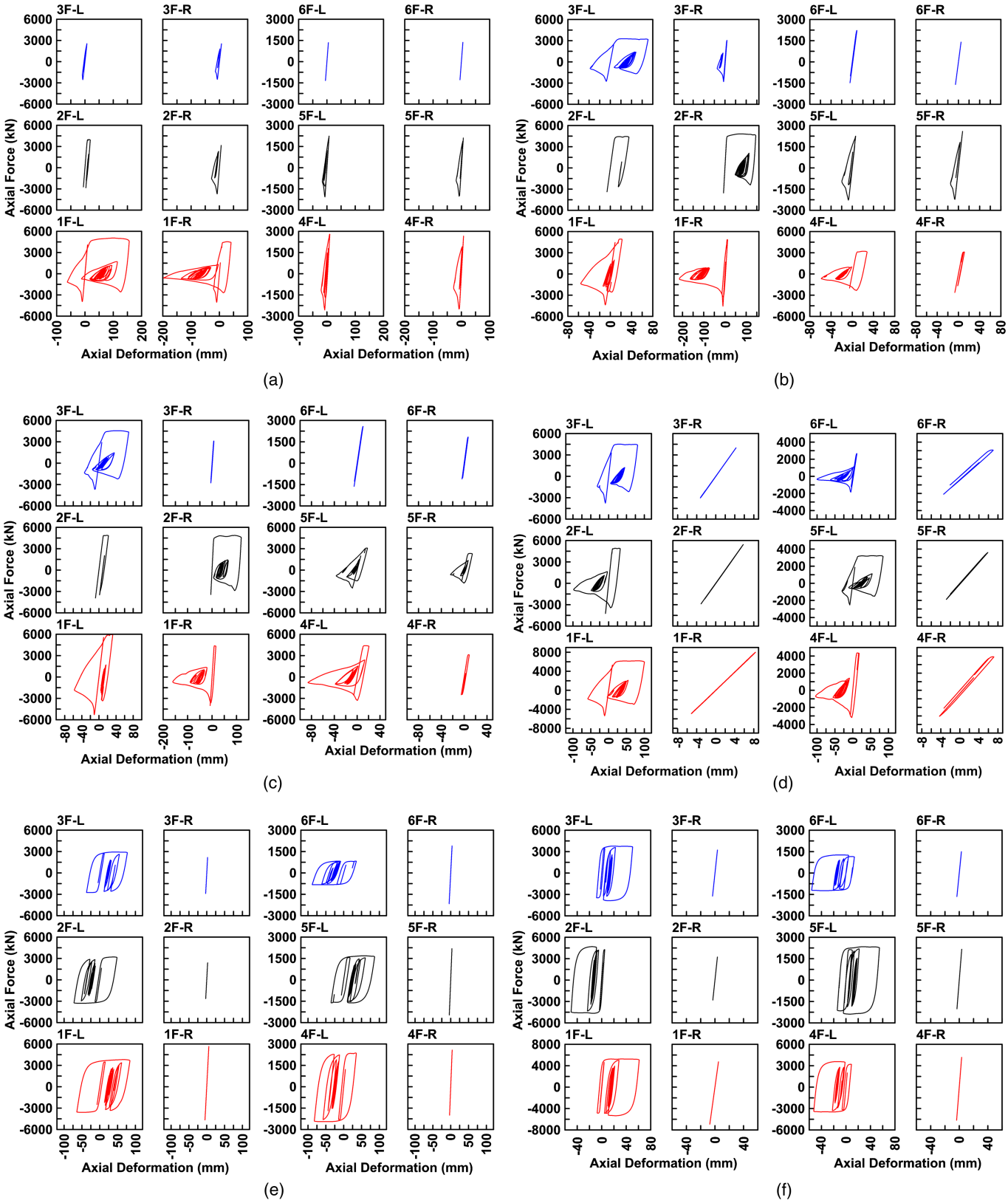

Fig. 12. Brace hysteretic responses of each model under scaled NGA 1602 fault-parallel component ground motion (MCE level): (a) V6; (b) X6; (c) X6-3; (d) SB6-3; (e) SB6-3B; (f) SB6-3 L

uniform distribution at the lower stories. All residual story drift ratios were less than 0.7%, as shown in Fig. 10. The residual story drift ratios under fault-parallel ground motions were all larger than that under fault-normal ground motions.

Dynamic Responses under Selected Ground Motion

Story drift ratio histories of each floor level and axial force-deformation relationships of all twelve braces for each model are shown in Figs. 11 and 12. Only the responses

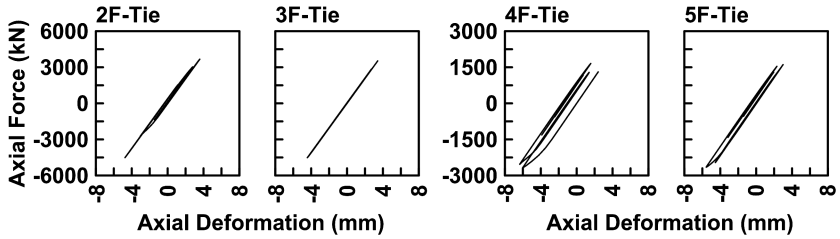

Fig. 13. Tie-columns hysteretic responses of SB6-3 model under scaled NGA 1602 fault-parallel component ground motion (MCE level)

selected from NGA-1602 fault-parallel component are shown herein.

From Figs. 11 and 12(a), it is clear that the deformation Model V6 experienced was concentrated at the first story. Localized concentration of deformation improved slightly in Model X6, where the lower stories tended to have higher story drift ratios and form a soft two-story-panel mechanism [Fig. 12(b)]. Model X6-3 responded similarly, but with the concentration of deformation slightly reduced, as shown in Fig. 12(c). Model SB6-3 successfully prevented localized concentration of story deformation. Most of the braces in the vertical spine remained elastic during the dynamic analyses, and all braces outside the spine were triggered to buckle, as shown in Fig. 12(d). Similar system responses were observed in Models SB6-3B and SB6-3 L. All BRBs deformed into the nonlinear range and exhibited stable hysteresis loops, as shown in Figs. 12(e and f). Significant strain hardening in the BRBs was observed. Most of the bracing members in the vertical spine remained elastic during the ground shaking.

In this MCE level ground motion event, the sixth story and fourth story braces in the vertical spine of Model SB6-3 exhibited nonlinear demands, as shown in right of Fig. 12(d). All of the lower three-story braces in the vertical spine remained elastic during the dynamic analyses. Buckling and yielding of tie-columns in the strongback vertical spine was also observed (Fig. 13).

Effect of Gravity Columns

All leaning columns in the *OpenSees* models were removed and the analyses performed again to examine the effects of gravity columns on response. The reanalysis results showed that the fundamental and the second-mode periods were essentially the same for all six models with or without leaning columns.

The mean responses of strongback models did not have significant changes when the gravity leaning columns were not included. The mean response did change significantly for the nonstrongback systems, however, as is evident by comparing Figs. 9, 10, 14, and 15, this is especially true when considering the maximum story drift ratio at each floor level. For example, the ground level maximum story drift ratio of nonstrongback systems (Models V6, X6, and X6-3) under MCE fault-parallel ground motions had 3–12% changes if excluding gravity columns in the models while the changes were less than 2% in strongback systems (Models SB6-3, SB6-3B, and SB6-3 L). The gravity columns did somewhat help on reducing deformation concentrations in the nonstrongback systems (Models V6, X6, and X6-3). The presence of leaning columns in the models had a significant effect on the residual story drift ratio at each floor level, as can be seen in Figs. 10 and 15. Basically, the maximum base shear forces, maximum roof displacements, and maximum column uplift forces were not affected by leaning columns. The peak axial deformations of braces were typically larger if the leaning columns were not modeled, and this phenomenon was more obvious in nonstrongback systems.

Cost Comparison

The steel weight of seismic force-resisting systems for each model was estimated to examine the increased initial construction costs as a result of introducing the strongback vertical spine and BRBs into the braced frame systems. The initial fabrication costs per tonnage steel was assumed to be US$3,300/t; the costs per BRB for the mid-rise building were assumed to be US$5,000/brace

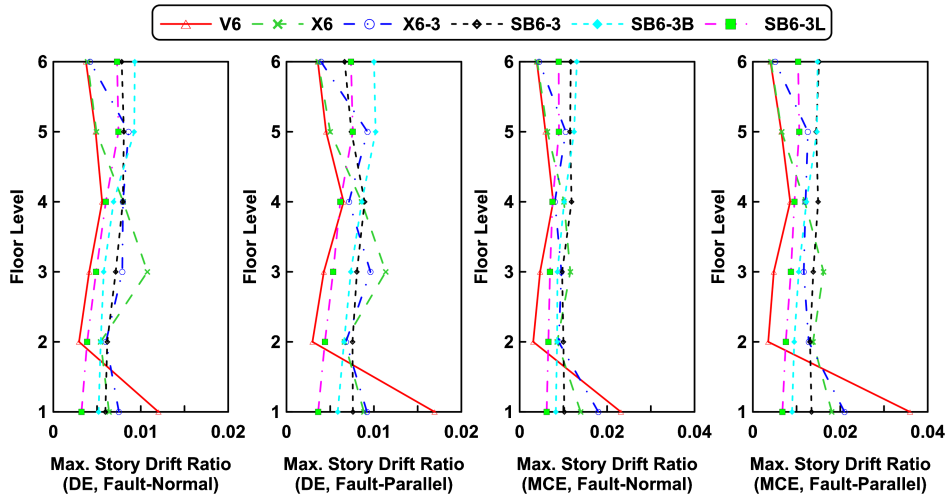

Fig. 14. Mean maximum story drift ratios for each model under DE and MCE level ground motions (without gravity columns)

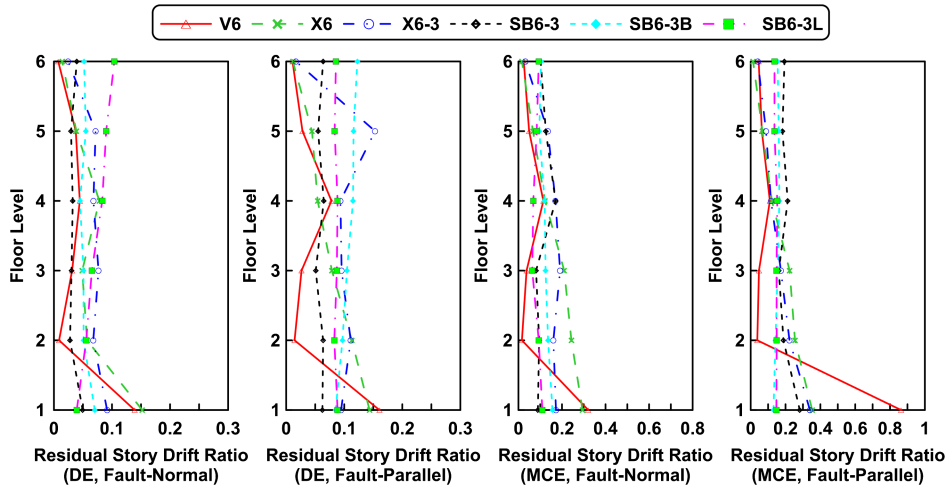

Fig. 15. Mean residual story drift ratios for each model under DE and MCE level ground motions (without gravity columns)

Table 7. Steel Weight Contributions and Estimated Initial Construction Cost for Each Model

Model	V6	X6	X6-3	SB6-3	SB6-3B	SB6-3 L
Column weight (tons)	80.8	80.8	80.8	80.8	80.8	80.8
Beam weight (tons)	83.9	31.0	31.0	31.0	31.0	31.0
Brace weight (tons)	26.4	26.4	29.8	36.7	17.3	17.3
Tie-columns weight (tons)	—	—	—	7.4	5.8	5.8
Connection equivalent weight (tons)	28.7	20.7	21.2	23.4	20.2	20.2
Number of buckling-restrained braces (BRB) used	—	—	—	—	24	24
BRB costs (US$)	—	—	—	—	120,000	240,000
Total weight w/o BRB (tons)	219.8	158.9	162.8	179.3	155.1	155.1
Total costs (US$)	725,430	524,370	537,240	591,690	631,830	751,830
Cost ratio	1.00	0.72	0.74	0.82	0.87	1.04

Note: Gravity columns and gravity beams are not included.

(DASSE 2009) and US$10,000/brace for regular-yield strength BRBs and low-yield-strength BRBs (including connection costs). The equivalent connection tonnage was assumed as 15% of steel weight (such as columns, beams, conventional braces, and tie-columns). Table 7 summarizes the weight and costs of each seismic force-resisting system.

From the cost ratios shown in Table 7, using strongback systems instead of chevron configuration braced frame (V6) could reduce the cost of seismic force-resisting system up to 18%. Compared with the estimated cost of the double-story X-braced frame (X6), the cost of using SBSs was about 13–43% higher.

Conclusions

The strongback system and a simple design strategy are proposed in this study with the goal of preventing deformation concentration in steel-braced frames. The performances of three conventional braced frame systems and three strongback systems were investigated using static pushover analyses and nonlinear dynamic response history analyses. Based on the extensive analysis results, the following conclusions can be drawn:

1. The proposed strongback system effectively prevented the soft-story mechanism in the braced frame systems.
2. The simplified design strategy that proportioned vertical spine member sizes in the strongback system achieved the key performance goal: uniform distribution of story deformation over height. Design optimization of this simple strategy should be studied further.
3. Compared with the conventional inverted-V braced frame (chevron configuration, Model V6), the strongback systems (Models SB6-3 and SB6-3B) not only performed better under selected ground motions, but they also cost about 13–18% less. For the strongback system using low-yield steel BRBs (SB6-3 L), the cost was about 4% more compared with the conventional inverted-V braced frame, however, peak transient drifts and residual displacements are reduced.
4. Although the effect of gravity columns on the dynamic responses was obvious in the nonstrongback systems, there were no significant effects found on the dynamic responses in the strongback systems. Gravity columns can help reduce deformation concentration but it is not considered a dependable or an efficient mechanism; the strongback is a preferred system to reduce deformation concentration.
5. Although using high-performance braces such as BRBs in the strongback system may further improve the deformation capacity of the entire system, larger residual deformations are expected to occur in upper levels of such hybrid braced frame systems. Using the devices with self-centering mechanisms would reduce the residual deformation.
6. The results indicate that the simple design strategy used does not result in adequate member sizes near the top of the strongback systems and limited yielding of the strongback spine occurs at these levels. Additional investigation is needed.

Acknowledgments

This research is supported by National Science Foundation (NSF) under grant number CMMI-0619161: International Hybrid Simulation of Tomorrow's Braced Frame Systems. Financial support from NSF is greatly appreciated. The conclusions and opinions expressed in this paper are those of the authors and do not necessarily represent the views of the sponsor.

References

American Institute of Steel Construction (AISC). (2005). "Seismic provisions for structural steel buildings." *AISC 341-05*, Chicago.

ASCE. (2005). "Minimum design loads for buildings and other structures." *ASCE 7-05*, Washington, DC.

Chen, C. H., and Mahin, S. A. (2012). "Performance-based seismic demand assessment of concentrically braced steel frame buildings." *PEER Rep. 2012/103*, Pacific Earthquake Engineering Research Center, Univ. of California, Berkeley, CA.

Clough, R. W., and Huckelbridge, A. A., (1977). "Preliminary experimental study of seismic uplift of a steel frame." *Rep. UCB/EERC-77/22*, Earthquake Engineering Research Center, Univ. of California, Berkeley, CA.

Computers, and Structures (CSI). (2009). "Integrated software for structural analysis and design." *SAP2000*, Berkeley, CA.

DASSE Design. (2009). "Cost advantages of buckling restrained braced frame buildings." San Francisco.

Deierlein, G., et al. (2011). "Earthquake resilient steel braced frames with controlled rocking and energy dissipating fuses." *Steel Constr. Des. Res.*, 4(3), 171–175.

Foutch, D. A., Goel, S. C., and Roeder, C. W. (1987). "Seismic testing of full-scale steel building—Part I." *J. Struct. Eng.*, 10.1061/(ASCE)0733-9445(1987)113:11(2111), 2111–2129.

Ghersi, A., Neri, F., and Rossi, P. P. (2000). "Seismic response of tied and trussed eccentrically braced frames." *Proc., Int. Workshop and Seminar on "behavior of steel structures in seismic areas"*, CRC Press/Balkema, Rotterdam, Netherlands.

Hines, E. M., and Appel, M. E. (2007). "Behavior and design of low-ductility braced frames." *Proc., Structures Congress: New Horizons and Better Practices*, ASCE, Reston, VA, 1–8.

Hines, E. M., Appel, M. E., and Cheever, P. J. (2009). "Collapse performance of low-ductility chevron braced steel frames in moderate seismic regions." *AISC Eng. J.*, 46(3), 149–180.

Kelly, J. M., and Tsztoo, D. F. (1977). "Earthquake simulation testing of a stepping frame with energy-absorbing devices." *Rep. UCB/EERC-77/17*, Earthquake Engineering Research Center, Univ. of California, Berkeley, CA.

Khatib, I. F., Mahin, S. A., and Pister, K. S. (1988). "Seismic behavior of concentrically braced frames." *Rep. UCB/EERC-88/01*, Earthquake Engineering Research Center, Univ. of California, Berkeley, CA.

Kiggins, S., and Uang, C.-M., (2006). "Reducing residual drift of buckling-restrained braced frames as a dual system." *Eng. Struct.*, 28(11), 1525–1532.

Lai, J.-W., Chen, C. H., and Mahin, S. A., (2010). "Experimental and analytical performance of concentrically braced steel frames." *Proc., Structures Congress*, ASCE, Reston, VA, 2339–2350.

Lopez, W. A., and Sabelli, R., (2004). "Seismic design of buckling-restrained braced frames." *Steel tips*, Structural Steel Education Council, Moraga, CA.

Mahin, S., and Lai, J. W. (2008). "An innovative approach to improving the seismic behavior of steel concentric braced frames." *Proposal for SEAONC Special Projects Initiative*, Univ. of California, Berkeley, Berkeley, CA.

Mar, D., (2010). "Design examples using mode shaping spines for frame and wall buildings." *Proc., 9th U.S. National and 10th Canadian Conf. on Earthquake Engineering*, Earthquake Engineering Research Institute, Oakland, CA.

Martini, K., Amin, N., Lee, P., and Bonowitz, D. (1990). "The potential role of non-linear analysis in the seismic design of building structures." *Proc., 4th U.S. National Conf. on Earthquake Engineering*, Earthquake Engineering Research Institute, El Cerrito, CA.

McKenna, F. (1997). "Object oriented finite element programming frameworks for analysis, algorithms and parallel computing." Ph.D. dissertation, Dept. of Civil and Environmental Engineering, Univ. of California, Berkeley, CA.

McKenna, F., Scott, M., and Fenves, G., (2010). "Nonlinear finite-element analysis software architecture using object composition." *J. Comput. Civ. Eng.*, 10.1061/(ASCE)CP.1943-5487.0000002, 95–107.

OpenSees version 2.2.2 [Computer software]. Berkeley, CA, Pacific Earthquake Engineering Research Center.

Popov, E. P., Ricles, J. M., and Kasai, K., (1992). "Methodology for optimum EBF link design." *Proc., 10th World Conf. on Earthquake Engineering*, CRC Press/Balkema, Rotterdam, Netherlands.

Rai, D. C., and Goel, S. C. (1997). "Seismic evaluation and upgrading of existing steel concentric braced structures." *Rep. UMCEE 97-03*, Dept. of Civil and Environmental Engineering, Univ. of Michigan, Ann Arbor, MI.

Robinson, K. (2009). "Specifying buckling-restrained brace systems." *Mod. Steel Constr.*, 49(11), 57–60.

Sabelli, R. (2001). "Research on improving the design and analysis of earthquake-resistant steel-braced frames." *2000 NEHRP Professional Fellowship Rep., PF2000-9*, Earthquake Engineering Research Institute, Oakland, CA.

Stavridis, A., and Shing, P. B. (2010). "Hybrid testing and modeling of a suspended zipper steel frame." *Earthquake Eng. Struct. Dyn.*, 39(2), 187–209.

Tirca, L., and Tremblay, R., (2004). "Influence of building height and ground motion type on the seismic behavior of zipper concentrically braced steel frames." *Proc., 13th World Conf. on Earthquake Engineering*, Vancouver, BC, Canada.

Tremblay, R. (2003). "Achieving a stable inelastic seismic response for multi-story concentrically braced steel frames." *AISC Eng. J.*, 40(2), 111–129.

Tremblay, R., and Merzouq, S., (2004). "Dual buckling restrained braced steel frames for enhanced seismic response." *Proc., Passive Control Symp.*, Tokyo Institute of Technology, Yokohama, Japan.

Uriz, P., and Mahin, S. A. (2008). "Toward earthquake-resistant design of concentrically braced steel-frame structures." *PEER Rep. 2008/08*, Pacific Earthquake Engineering Research Center, Univ. of California, Berkeley, CA.

Whittaker, A. S., Uang, C.-M., and Bertero, V. V., (1990). "An experimental study of the behavior of dual steel systems." *Rep. UCB-EERC-88/14*, Earthquake Engineering Research Center, Univ. of California, Berkeley, CA.

Yang, C. S., Leon, R. T., and DesRoches, R., (2008). "Pushover response of a braced frame with suspended zipper struts." *J. Struct. Eng.*, 10.1061/(ASCE)0733-9445(2008)134:10(1619), 1619–1626.

Yang, C. S., Leon, R. T., and DesRoches, R., (2010). "Cyclic behavior of zipper-braced frames." *Earthquake Spectra*, 26(2), 561–582.

Yang, T. Y., Stojadinovic, B., and Moehle, J. (2009). "Hybrid simulation of a zipper-braced steel frame under earthquake excitation." *Earthquake Eng. Struct. Dyn.*, 38(1), 95–113.